Investigation of the drug release time from the biodegrading coating of an everolimus eluting stent

Dimitrios S. Pleouras, Georgia S. Karanasiou, Vasileios S. Loukas, Arsen Semertzioglou, Anargyros
N. Moulas and Dimitrios I. Fotiadis, *Fellow, IEEE*

Abstract — This case-study examines the release time of the everolimus drug from an experimental biodegrading coating of a Rontis corp. drug eluting stent (DES). The controlled drug release is achieved by the degradation of the coating, which consists of a mixture of polylactic co-glycolic acid (PLGA) and everolimus (55:45). In our analysis, we used the outcome of another study, which contains the geometry of an *in-silico* deployed Rontis corp. stent in a 3D reconstructed coney arterial segment. Using this geometry as input, the everolimus release was simulated using a computational model that includes: i) modeling of the blood flow dynamics, ii) modeling of PLGA degradation, and iii) modeling of the everolimus advection and diffusion towards both the lumen and the arterial wall. The results show the rapid release of everolimus. This is justified due to the high porosity of the coating, which is caused by the initial high concentration of everolimus in the coating.

Clinical Relevance — The methodology presented in this work is an additional step towards predicting accurately drug release from DES. Also, the results of our work prove that high drug concentration in the coating causes its rapid release, which could be used as input in the design of new DES.

I. INTRODUCTION

Since the beginning of the 21st century, cardiovascular disease (CAD) remains the leading cause of death worldwide, according to the World Health Organization (WHO) [1]. Atherosclerosis is the dominant cause of CAD, and therefore it is a major research focus of several studies [2]. Atherosclerosis is identified by the development of plaque within the arterial walls, which causes arterial wall thickening and subsequently, lumen narrowing, and may lead eventually to cardiovascular events. Over the past century, the major risk factors of CAD have been discovered, identifying high serum lipids, smoking, diabetes and obesity as the major culprits of atherosclerosis [3]. Nowadays, atherosclerosis can be prevented either by regulating the patient's diet and exercise program, or by providing medications to lower the serum lipids. However, in the case of a cardiovascular event, blood flow in the throttled arteries can only be restored by invasive techniques, such as percutaneous coronary revascularization (balloon angioplasty or stent deployment) and coronary artery bypass.

Percutaneous coronary revascularization by balloon angioplasty was first introduced in 1977 by Gruentzig. Although remarkable as a discovery, balloon angioplasty is prone to coronary dissections, arterial recoil and neointima formation [4]. Endoluminal coronary stenting was realized nine years later in 1986 by Ulrich Sigwart to prevent the elastic recoil of the throttled vessel and limit the arterial dissections [5]. However, the stenting procedure did not resolve the problem of neointima formation that results in restenosis. Neointima formation develops from damage in the arterial wall and it is caused by smooth muscle cells' accumulation in the intima region of the vessel. At the beginning of this century, drug eluting stents (DES) were developed to avoid restenosis, which gradually release medication to inhibit restenosis [6].

Several studies were performed to investigate the risks of the first generation DES deployment, which showed the delayed re-endothelialization of the treated vessel that eventually lead to high rates of myocardial infraction and late thrombosis after the dual antiplatelet therapy (DAPT) ends [7]. To address this issue, researches developed the second generation of DES in 2016 having the desired features regarding biocompatibility. More specifically, these features include biocompatible materials, such as cobalt-chromium, platinum-chromium and cobalt-nickel alloys for the stents's metal core, while polylactic acid and polylactic-co-glycolic acid for the polymeric coatings. Moreover, better stent designs were developed to respond better in stretching, while being thinner to allow for a faster re-endothelization.

The significant factor of a DES drug release rate had been regulated by modeling approaches, which enabled the prediction of the drug release from the deployed stents in order to eliminate the cases of high and low drug concentrations in the arterial wall, leading to toxicity or restenosis respectively. One of the first modeling approaches was provided by Zunino *et al*. in 2009, who performed a 2D case study of the heparin drug release from the coating surface towards the adventitia layer of the porous arterial wall using the advection-diffusion equation for drug release and Darcy's law for the momentum losses due to porosity [8]. A more complicated geometry of the arterial wall, was examined by both Pontrelli and de Monte in 2010, and McGinty *et al.* in 2011, where at least 3 layers of the arterial wall were considered in their drug release analyses [9], [10]. In 2013, O'Brien *et al*. performed a 2D analysis of the stent coating's drug release towards both the lumen and the arterial wall, taking into consideration the pulsatile blood flow

D.S. Pleouras, G.S. Karanasiou, Vasileios S. Loukas and D.I. Fotiadis are with the Unit of Medical Technology and Intelligent Information Systems, Department of Materials Science and Engineering, University of Ioannina, Ioannina, GR 45110 Greece.

D.I. Fotiadis is also with the Dept. of Biomedical Research, FORTH-IMBB, GR 45110 Ioannina, Greece (corresponding author phone: +302651009006; fax: +302651008889; e-mail: fotiadis@uoi.gr).

A.N. Moulas is with the Dept. of Agricultural Technology, University of Thessaly, Lamia, GR 35100 Greece.

A Semertzioglou is with the Rontis Corporation S.A., Greece

[11]. Drug elution models were refined by Zhu *et al*. in 2014, who used an analytical model for the coating's polymerization resulting in a transient porosity, as well as a transient diffusivity for the studied drug. In their approach, the drug binding in the arterial wall was also considered [12]. A realistic case study was performed by Rikhtegar *et al*., which includes the geometry of a deployed stent in a 3D reconstructed arterial segment [13]. In 2016, Saha and Mandal investigated the effect of the struts' distance on the distribution of the free and the bound drug in the arterial wall by performing a parametric analysis [14]. Saha and Mandal performed another study, in which they used their previous model and extended it to include the pulsatile blood flow and an atherosclerotic area in the arterial wall [15]. Further efforts involve the drug binding into specific and non-specific receptors in the arterial wall, as proposed by Tzafriri *et al*. [16], as well as the shrinking coating based on polymerization, as proposed by Vo *et al*. [17]. The majority of these studies utilized either 2D or 3D idealized and non-realistic arterial geometries.

This study examines the transient release of the drug everolimus from the polylactic co-glycolic coating of a Rontis corp. stent, which was previously deployed *in silico* in a realistic 3D reconstructed coney arterial segment. This is achieved using a modeling approach that includes an analytical model for the PLGA degradation, which is based on the polymerization process as proposed by Zhu *et al*., and an explicit model for the everolimus release towards both the lumen and the porous arterial wall due to advection and diffusion forces. To the best of our knowledge, this is the first study that applies a detailed drug release model to the resulted geometry of an *in silico* deployment of a DES in a 3D reconstructed coney arterial segment.

II. MATERIAL AND METHODS

A. Dataset

Despite the majority of the drug delivery modeling studies that implement ideal 2D or 3D arterial data, this work uses real coney arterial imaging from the BioCoStent study. Specifically, the BioCoStent study provides optical coherence tomography (OCT) imaging data from coney coronary arterial segments. The OCT imaging data include information of the lumen border as well as the adventitia border, which can be used to reconstruct the arterial segment using a straight line as the arterial centerline. In the case of existent corresponding angiography data, the arterial centerline can be properly calculated.

B. 3D reconstruction of coronary arteries

The 3D reconstruction of the OCT imaging was performed using an in house 3D reconstruction tool [18]. In brief, the 3D reconstruction methodology can be separated in the pre-processing of the imaging data, that includes both the removal of the blooming effect caused by the calcified plaques and the identification of the potential vessel borders, as well as the segmentation, which is enabled using a 3D level set algorithm.

C. In-silico deployment of drug eluting stent

To maintain the integrity of the study, instead of virtually deforming the drug eluting stent to fit into the reconstructed arterial segment, it was deployed *in-silico* using an already
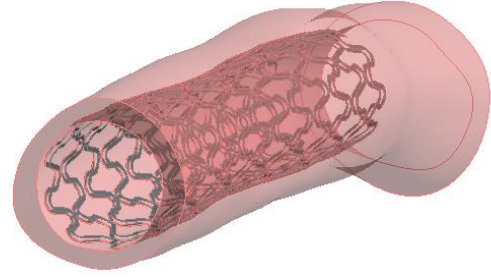

Figure 1. The resulted geometry of the arterial wall and the deployed stent, which is used as an input to this analysis [20].

developed mathematical model [19]. This step is necessary to maintain the realism of this case-study. Figure 1 illustrates the in silico deployed stent in the reconstructed arterial segment.

D. Drug delivery model

Drug elusion is predicted using the presented computational model that includes the blood flow in the lumen and the arterial wall, the degradation of the polymeric coating and the transient drug release towards the lumen and the arterial wall by diffusion and advection forces.

The coating of the examined stent contains everolimus at 45% w/w, resulting in an everolimus concentration of 563.55 mol/m^3 using Eq. 1. In addition, the porosity of the polymer can be calculated using Eq. 2.

$$C_{drug}\left(\frac{mol}{m^3}\right) = Ratio_{drug}\left(\frac{w}{w}\right) * \frac{\rho_{PLA}\left(\frac{g}{m^3}\right)}{MW_{drug}\left(\frac{g}{mol}\right)}, \quad (1)$$

$$\varphi_0 = Ratio_{drug}\left(\frac{w}{w}\right) * \frac{\rho_{drug}\left(\frac{g}{m^3}\right)}{\rho_{PLA}\left(\frac{g}{m^3}\right)}, \quad (2)$$

where C_{drug} is the molar concentration of the drug, $Ratio_{drug}$ is the mass percentage of the drug in the coating, ρ_{PLA} is the density of the PLA ($\rho_{PLA} = 1.2$g/cm^3 [20]), MW_{drug} is the molecular weight of the drug ($MW_{everolimus} = 958.2$ g/mol [21]), ρ_{drug} is the density of the drug ($\rho_{everolimus} = 1.2$ g/cm^3 [22]) and φ_0 is the coating's initial porosity due to the presence of the drug ($\varphi_0 = 0.45$).

The release of everolimus from the polymeric coating is based on diffusion forces (Eq. 3). However, the degradation of the polymer creates an altering environment in the coating, where the coating's porosity gradually increases and affects the diffusivity of everolimus. Therefore, the equation of the active diffusivity is used for everolimus (Eq. 4) instead of a steady term, that considers both the diffusivity of the porous and the solid phase (Eq. 5) of the coating [12].

$$\frac{\partial C_{drug}}{\partial t} = \frac{\partial}{\partial x_i}\left(D_e(MW,\varphi)\frac{\partial C_{drug}}{\partial x_i}\right), \quad (3)$$

$$D_e = \frac{(1-\varphi)D_s + \kappa\varphi D_l}{1-\varphi+\kappa\varphi}, \quad (4)$$

$$D_s = D_{s0}\left(e^{-k_w t}\right)^{-a}, \quad (5)$$

$$\varphi = \varphi_0 + (1-\varphi_0)(1 + e^{-2kt} - 2e^{-kt}), \quad (6)$$

where D_e is the active diffusivity of everolimus, D_s is the diffusivity of everolimus in the solid phase, D_l is the diffusivity of everolimus in the porous regions that are filled with blood (D_l = 0.985μm²/s [23]), D_{s0} is the initial diffusivity of everolimus in the non-degraded polymer (D_{s0} = 0.0224μm²/s [23]), k_w is the molecular degradation rate of the polymer (k_w = 2.5x10⁻⁷ 1/s [12]), a is a parameter for the molecular weight change model (a = 1.714 [24]) and φ is the coating's porosity.

In the domains of the lumen and the arterial wall, drug transport depends also on advection forces. The blood flow in the lumen is laminar, incompressible and Newtonian, which can be described by the Navier-Stokes equations (Eq. 7-9), while the released everolimus in the lumen can be described by the advection-diffusion equation (Eq. 10) [25].

$$\rho\frac{\partial U_j}{\partial t} + \frac{\partial}{\partial x_i}\left(\rho U_i U_j\right) = -\frac{\partial P}{\partial x_j} - \frac{\partial \tau_{ij}}{\partial x_i}, \tag{7}$$

$$\tau_{ij} = -\mu\left(\frac{\partial U_j}{\partial x_i} + \frac{\partial U_i}{\partial x_j} + \frac{2}{3}\delta_{ij}\mu\frac{\partial U_k}{\partial x_k}\right), \tag{8}$$

$$\frac{\partial(\rho U_i)}{\partial x_i} = 0, \tag{9}$$

$$\frac{\partial C_{drug}}{\partial t} + \frac{\partial}{\partial x_i}\left(U C_{drug}\right) = \frac{\partial}{\partial x_i}\left(D_l\frac{\partial}{\partial x_j}C_{drug}\right). \tag{10}$$

where U, ρ, P and μ are the velocity, the density, the pressure and the viscosity of blood (ρ = 1060 kg/m³ [26], μ = 0.0035 Pa s [27]), respectively, while τ is the shear stress tensor and δ is the Kronecker delta.

In the porous arterial wall, blood's plasma enters through endothelium and flows in between the cells' interspace. The blood and plasma have almost equal transport properties, and therefore, in our analysis, we assume them as a single liquid. The plasma flow is described by the modified Navier-Stokes equations (Eq. 11-15), while everolimus transport is described by the modified advection-diffusion equation (Eq. 16). These equations are modified to account for the momentum loss due to the porosity of the arterial wall [25].

$$\rho\gamma\frac{\partial U_j}{\partial t} + \frac{\partial}{\partial x_i}\left(\rho(\boldsymbol{K}\cdot\boldsymbol{U})_i U_j\right) = -\gamma\frac{\partial P}{\partial x_j} - \frac{\partial \tau_{ij}}{\partial x_i} + S_{M,i}, \tag{11}$$

$$where, \quad \tau_{ij} = -\mu\left(\frac{\partial U_j}{\partial x_i} + \frac{\partial U_i}{\partial x_j} + \frac{2}{3}\delta_{ij}\mu\frac{\partial U_k}{\partial x_k}\right), \tag{12}$$

$$K^{ij} = \gamma\delta^{ij}, \tag{13}$$

$$S_{M,i} = -\frac{\mu}{K_{perm}}\boldsymbol{U}_i, \tag{14}$$

$$\frac{\partial(\rho\boldsymbol{K}\cdot\boldsymbol{U})_i}{\partial x_i} = 0, \tag{15}$$

$$\gamma\frac{\partial C_{drug}}{\partial t} + \frac{\partial}{\partial x_i}\left((\boldsymbol{K}\cdot\boldsymbol{U})_j C_{drug}\right) = D_l\frac{\partial}{\partial x_i}\left(\boldsymbol{K}\cdot\frac{\partial}{\partial x_j}C_{drug}\right), \tag{16}$$

where, $\boldsymbol{K}$ is the area porosity tensor, γ is the volume porosity, S_M is the momentum losses due to porosity, everolimus in the solid phase and K_{perm} is the Darcian permeability.
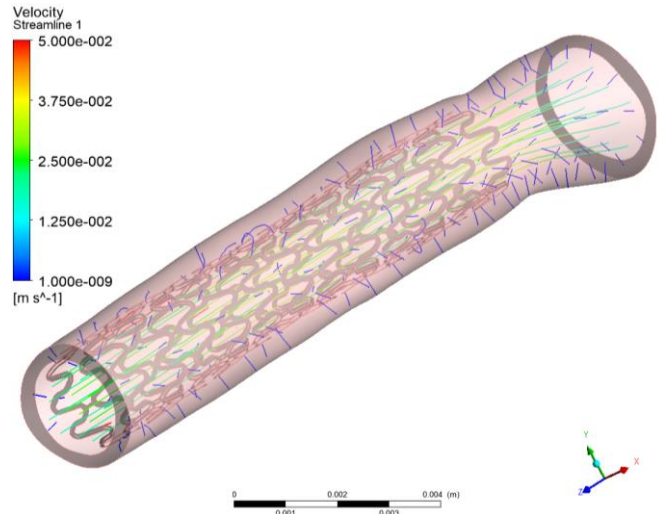

Figure 2. The simulated streamlines, colored according to the magnitude of the velocity.

III. RESULTS & DISCUSSION

Our analysis is realistic as we used as an input the presented model the *in-silico* deployed stent in a reconstructed coney arterial segment as it resulted from [19]. The timeframe of our analysis considers one month, while each timestep consists of 4 hours. Figure 2 illustrates the simulated streamlines in the domains of the lumen and the arterial wall. The flow velocity in the arterial wall is nine orders of magnitude larger than in the lumen domain, which is in agreement with other works [25]. Figure 3 shows the everolimus distribution of the arterial wall in 4 different time-points at the period of 0-24 hours. It shows a sharp increase of the everolimus concentration in the arterial wall at the first 8 hours, as well as, a subsequent sharp decrease, that proves the rapid release of the drug from the stent's coating. This is also observed in the Figure 4, which shows the rapid release of everolimus as a function of its mass fraction in the coating in relation to time.
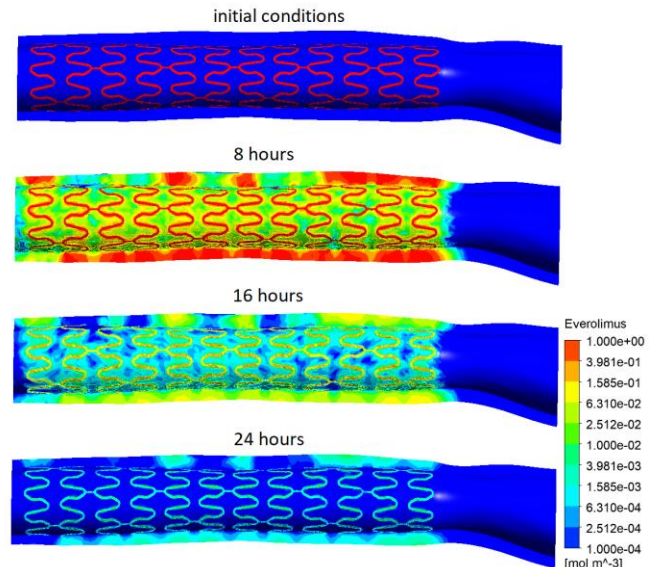

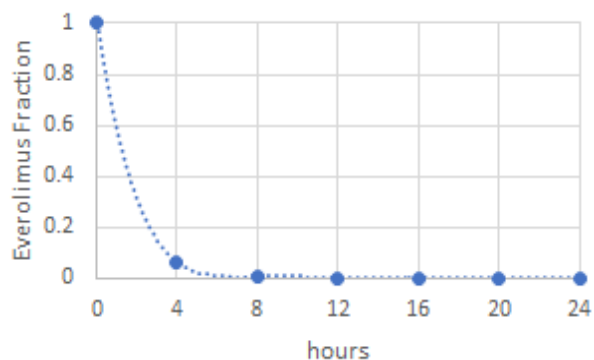Figure 3. Everolimus distribution in the arterial wall at 8-hour intervals.

Figure 4. The fraction of the remaining everolimus in the stent coating in relation to time.

In this case-study, the resulted drug release rate is much larger from the corresponding ones presented in most DES studies, where the complete drug release requires three to six months of time [17]. However, short release periods have also been observed and studied [10]. In relation to other DES, our case differs in the initial drug concentration in the coating. Specifically, in this study, the initial everolimus concentration of the coating was 45% w/w, which is much larger than in other DES [12]. To the best of our knowledge, such a coating drug concentration has never been examined before as a possible solution to prolong the drug elusion period. However, the results showed that the high initial drug concentration requires a low polymer concentration in the mixture, resulting in a highly porous coating, which favors the drug release rates. Therefore, the high drug concentration leads to rapid release, instead of a prolonged one in homogeneous coating mixtures.

Last, another novelty of this work, is that it uses the geometry of an *in silico* deployed DES in a 3D reconstructed coney arterial segment as an input to a detailed drug release model that couples a polymer degradation model and a model for drug release towards both the lumen and the arterial wall.

REFERENCES

[1] "The top 10 causes of death." https://www.who.int/news-room/fact-sheets/detail/the-top-10-causes-of-death (accessed Jan. 13, 2021).

[2] J. Frostegård, "Immunity, atherosclerosis and cardiovascular disease," p. 13, 2013.

[3] P. Libby, "History of Discovery: Inflammation in Atherosclerosis," p. 15, 2013.

[4] T. Simard, B. Hibbert, F. D. Ramirez, M. Froeschl, Y.-X. Chen, and E. R. O'Brien, "The Evolution of Coronary Stents: A Brief Review," *Canadian Journal of Cardiology*, vol. 30, no. 1, pp. 35–45, Jan. 2014, doi: 10.1016/j.cjca.2013.09.012.

[5] A. Roguin, "Stent: The Man and Word Behind the Coronary Metal Prosthesis," *Circ Cardiovasc Interv*, vol. 4, no. 2, pp. 206–209, Apr. 2011.

[6] C.-W. Hwang, D. Wu, and E. R. Edelman, "Physiological Transport Forces Govern Drug Distribution for Stent-Based Delivery," *Circulation*, vol. 104, no. 5, pp. 600–605, Jul. 2001.

[7] A. V. Finn *et al.*, "Vascular Responses to Drug Eluting Stents," p. 11.

[8] P. Zunino, C. D'Angelo, L. Petrini, C. Vergara, C. Capelli, and F. Migliavacca, "Numerical simulation of drug eluting coronary stents: Mechanics, fluid dynamics and drug release," *Computer Methods in Applied Mechanics and Engineering*, vol. 198, no. 45–46, pp. 3633–3644, Sep. 2009.

[9] G. Pontrelli and F. de Monte, "A multi-layer porous wall model for coronary drug-eluting stents," *International Journal of Heat and Mass Transfer*, vol. 53, no. 19–20, pp. 3629–3637, Sep. 2010.

[10] S. McGinty, S. McKee, R. M. Wadsworth, and C. McCormick, "Modelling drug-eluting stents," *Mathematical Medicine and Biology*, vol. 28, no. 1, pp. 1–29, Mar. 2011.

[11] C. C. O'Brien, V. B. Kolachalama, T. J. Barber, A. Simmons, and E. R. Edelman, "Impact of flow pulsatility on arterial drug distribution in stent-based therapy," *Journal of Controlled Release*, vol. 168, no. 2, pp. 115–124, Jun. 2013, doi: 10.1016/j.jconrel.2013.03.014.

[12] X. Zhu, "Mathematical Modeling and Simulation of Intravascular Drug Delivery from Drug-Eluting Stents with Biodegradable PLGA Coating," p. 190.

[13] F. Rikhtegar, E. R. Edelman, U. Olgac, D. Poulikakos, and V. Kurtcuoglu, "Drug deposition in coronary arteries with overlapping drug-eluting stents," *Journal of Controlled Release*, vol. 238, pp. 1–9, Sep. 2016.

[14] R. Saha and P. K. Mandal, "Effects of Interstrut Distance on the Transport of Drug and its Retention in the Arterial Tissue," *Int. J. Appl. Comput. Math*, vol. 3, no. 3, pp. 2039–2054, Sep. 2017, doi: 10.1007/s40819-016-0223-2.

[15] R. Saha and P. K. Mandal, "Effect of flow pulsatility and time-dependent release kinetics on stent-based delivery through atherosclerotic plaque," *Int. J. Dynam. Control*, vol. 6, no. 1, pp. 1–13, Mar. 2018.

[16] A. R. Tzafriri *et al.*, "Defining drug and target protein distributions after stent-based drug release: durable versus deployable coatings," *Journal of Controlled Release*, p. 21, Feb. 2018.

[17] T. T. N. Vo, S. Morgan, C. McCormick, S. McGinty, S. McKee, and M. Meere, "Modelling drug release from polymer-free coronary stents with microporous surfaces," *International Journal of Pharmaceutics*, vol. 544, no. 2, pp. 392–401, Jun. 2018.

[18] V. I. Kigka *et al.*, "3D reconstruction of coronary arteries and atherosclerotic plaques based on computed tomography angiography images," *Biomedical Signal Processing and Control*, vol. 40, pp. 286–294, Feb. 2018.

[19] V. Loukas *et al.*, "Investigation of Drug Eluting Stents Performance Through in silico Modeling," 2021, pp. 712–721.

[20] "Polylactic acid," *Wikipedia*. Jan. 09, 2021, Accessed: Jan. 27, 2021. [Online]. Available: https://en.wikipedia.org/w/index.php?title=Polylactic_acid&oldid=999321981.

[21] PubChem, "Everolimus (RAD001)." https://pubchem.ncbi.nlm.nih.gov/compound/46930999 (accessed Jan. 27, 2021).

[22] "Retinoic acid | C20H28O2 | ChemSpider." https://www.chemspider.com/Chemical-Structure.50645001.html?rid=bae0c136-c181-43fb-a77e-cf08824badcb&page_num=0 (accessed Oct. 23, 2020).

[23] S. Hossainy and S. Prabhu, "A mathematical model for predicting drug release from a biodurable drug-eluting stent coating," *J. Biomed. Mater. Res.*, vol. 87A, no. 2, pp. 487–493, Nov. 2008, doi: 10.1002/jbm.a.31787.

[24] X. Zhu and R. D. Braatz, "A mechanistic model for drug release in PLGA biodegradable stent coatings coupled with polymer degradation and erosion: A Mechanistic Model for Drug Release in PLGA," *J. Biomed. Mater. Res.*, vol. 103, no. 7, pp. 2269–2279, Jul. 2015, doi: 10.1002/jbm.a.35357.

[25] D. S. Pleouras *et al.*, "Simulation of atherosclerotic plaque growth using computational biomechanics and patient-specific data," *Sci Rep*, vol. 10, no. 1, p. 17409, Dec. 2020, doi: 10.1038/s41598-020-74583-y.

[26] U. Olgac, V. Kurtcuoglu, and D. Poulikakos, "Computational modeling of coupled blood-wall mass transport of LDL: effects of local wall shear stress," *American Journal of Physiology-Heart and Circulatory Physiology*, vol. 294, no. 2, pp. H909–H919, Feb. 2008.

[27] M. I. Papafaklis, C. V. Bourantas, P. E. Theodorakis, C. S. Katsouras, D. I. Fotiadis, and L. K. Michalis, "Relationship of shear stress with in-stent restenosis: Bare metal stenting and the effect of brachytherapy," *International Journal of Cardiology*, vol. 134, no. 1, pp. 25–32, May 2009, doi: 10.1016/j.ijcard.2008.02.006.